MATHEMATICAL EQUATIONS ON KINEMATIC THEORY FOR ROBOTIC APPLICATIONS

B.RAMADEVI
Assistant professor
S&H MATHEMATICS
St Martin's Engineering College, Dhulapally
Pin : 500100
ramyasrinu26@gmail.com

Abstract: *This approach was proposed as a solution to enhancement of efficiency, reliability and dynamic environment for large-scale complex systems. The cinematic approach facilitates dynamic body movement which can replicate the fluid flow pressure field which induces undulatory movement of fish. Moreover, the research of cinematics and dynamics led to the statistical formulation of the fish body movement that explains its fluid behaviour. The study focuses on designing a linear system model with a derivation of robot dynamics owing to the complexities of the mechanical system. In this context we have compared other mathematical functions to see their potential to replace robot rectilinearly swimming on a two-dimensional basis with a better undulatory wave function.*

Key words: Mathematical equations, Kinematic theory, robotic applications.

1.0 Introduction

Biomimetics [1] Reflects the biological engineering characteristics and capabilities [2] of a system that can be effectively replicated and mi micronized in a human environment for developing and enhancing new technologies. Some of the benefits of integral forms is that it has a well-defined value in the quantity, and is also used in computational calculations, such as finite quantity methods. The advantage of writing this in terms of a differential equation is that we can use all the solutions available to solve the interest problem. Such two forms are naturally closely related and can also be transformed between them. But physical rules or properties may also be represented implicitly by interconnected equations. Examples include reverse problems, non-local problems and problems of viscoelasticity and creep.

The kinematics-based approach allows a dynamical movement of the body to replicate the fluid pressure field that produces the fish's undulating action. The cinematic and dynamic work also helped shape the quantitative model of fish body motions that defined their complex behaviour. From a robot viewpoint, it is still a big issue in the study of robotic fish to identify and increase swim capacity. The robot fish swimming like a genuine fish however does not guarantee the same high efficiency [3]. Multiple works have highly mentioned the undulatory (oscillatory) nature of the fish motion [4]. Researchers [5-8] are also able to carry

out a large number of experimentations and find empirical terms to refine the movement functions of the body and finish propulsion.

Objectives

- Each wave feature of bio inspiration incorporates a trajectory programmed by reverse cinematics, resulting in a bio-inspired algorithm to generate laterally compact caudal area waveforms.
- Integration with the current bio-inspired algorithms deriving out of various mathematical inputs of the present paradigm for robotic fish (kinematics and dynamics).
- Finding the operating part (ORE) for the identified kinematic parameter to facilitate closed-loop controller based on the characterization of the biological fish swimming model.

2.0 Methodology and equations

The BCF-mode locomotive carangi-size[5] is approximated using a two-sided joint structure (including pectorals connected to the head) as shown in Figure 1. As the "arm" and the second relation as the leg, the first connection is around two thirds of the total robot length. The robot tail is shaped by the caudal fin's third component. The design of the fish with the non-fixed head is seen. Our 3-link system (n = 2), which is an appropriate approximation to the BCF carangiform locomotive, can also be used in a carangiform swimming study with a limited number of modifications to this layout. Furthermore, a thunny (shark) half-growth system has been converted into a caudal peduncle and perfect to provide an effective thrust, allowing fast cruise speed for an extended period of time[5]. Although the cinematics research describes the geometry of robotic fish motion, a stationary coordinate frame can be defined entirely by translating the centroid and the rotation of the body around the centroid [10-12] as a function of the periods, in order to decide the dynamics of any hard body .

The dynamics of kinetic and potential energies produce free flow water in the robotic fish network in any relation and inertia. The interlinking actuator shaft reflects the inertial frame of reference when explaining the film and dynamics of the model seen in Figure 1. Each degree of freedom (DOF) is given a local coordinate system.

$$\frac{d}{dt}\left(\frac{\partial L}{\partial \dot{q}_i}\right)-\frac{\partial L}{\partial q_i}=\tau_i \quad i=1,2,\ldots,n$$

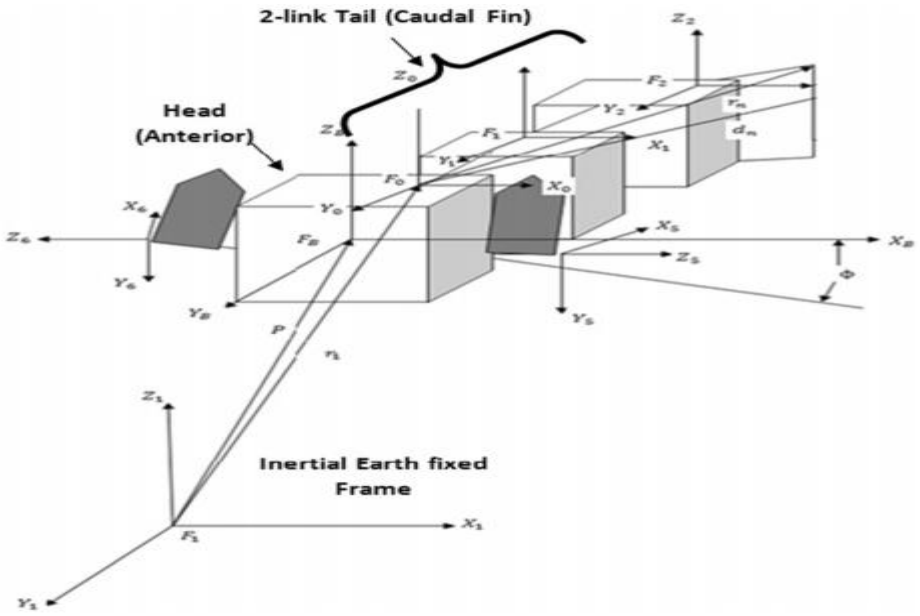

Figure 1 Relative orientations and localisation of local coordinate frames at CM of the point and inertial earth-fixed reference frame.

The Lagrange (L) function is defined as the difference between the kinematic and potential energies expressed as: L = K−P

Where K is the robot's total kinetic power; P is the robot's overall potential energy; qi is the ith coordinate variable joint; qi is the first time ith joint vector and ći is the equivalent generalized force (external torque) at the ith joint working at the head. For an N-link manipulator on a 6-DOF basis, the dynamic equations of the manipulator were built in three dimensions, given there is gravity operating on the structure. The travel equations for the existing 2-link robotic fish based on the n-link serial handler can be set as follows:

$$\sum_{j=1}^{n} D_{ij}(q)\ddot{q}_j + \sum_{k=1}^{n}\sum_{m=1}^{n} h_{ikm}\dot{q}_k\dot{q}_m + c_i = \tau_i \qquad i = 1, 2 .., n$$

where D(q) is the symmetrical matrix of inertia, hqð al; q is the momentum coupling function or Coriolis and the centrifugal force vector; c(q) is the function of gravity, and Ś is the total power of the equations of Lagrange.

In the small peduncle area maximally the wave amplitude even decreases from head to tail. Light hill generalized the slender body hypothesis in his study of Gray's work, which suggested that the total body fluid flux is a part of the constant stream along the straight body and the stream due to a side displacement of h(x, t). The second factor (flow) V(x, t) for a particular transverse section area Sx with fluid speed U, as indicated

$$V(x,t) = \left(\frac{\partial h}{\partial t}\right) + U\left(\frac{\partial h}{\partial x}\right)$$

The overall swimming efficiency as a function of overall fluid flow V(x, t) is termed as Froude's efficiency

$$\eta_f = 1 - \frac{1}{2}\left[\frac{V(x,\bar{t})^2_{x=l}}{\left(\frac{\partial h}{\partial t}\right)V(x,t)_{x=l}}\right]$$

In addition to endorsing a compact lateral wave and preserving a high output of Froude (as can be achieved by organic fish), Light thill proposed the action of the traveling wave displacement vector h(x, t) as an analytical expression.

$$h(x,t) = f(x) \times g(t - x/c)$$

Where the f(x) term for the amplitude is a wave-dependent oscillatory frequency feature and the fish body velocities, g[x, t] are planned to measure the efficacy of cubic polynomials for each rotational joint and also more specifically to lateral displacement data points, modeling continuous and smooth (non-jerky) motions. More intermediate, or by aircraft stages, may also be used. Cube polynomials have been documented in the field of trajectory generation for robotics, owing to their ability to control complex journeys efficiently.

$$y_{body}(x,t) = \left[\left(c_1 x + c_2 x^2 + c_3 x^3\right)\right]\left[\sin(kx + 2\pi f \times t)\right]$$

These variables make the resulting trajectory smooth over a given time where the direction, inclination and elevation are changing slowly. Physically speaking, this smoothness ensures that the power supply of the robot network switches less suddenly which decreases navigational errors which helps to limit the power usage of the robot.

Undulatory motions defined by the function in two degree and three-degree NURB equations are written as:

$$y_{body}(x,t) = \left\{\frac{c_1 x + c_2 x^2}{\sqrt{{c_1}^2 + {c_2}^2}}\right\}\sin(kx + 2\pi f \times t)$$

$$y_{body}(x,t) = \left\{\frac{c_1 x + c_2 x^2 + c_3 x^3}{\sqrt{{c_1}^2 + {c_2}^2 + {c_3}^2}}\right\}\sin(kx + 2\pi f \times t)$$

Most waveforms show a smooth curvature, suggesting unaffected oscillation / adulator (except for the two (quadratic and cubic) splines Bezier. This effect induces the undesirable offset deviation from the real trajectory points of the target control points.

3.0 Results and discussions

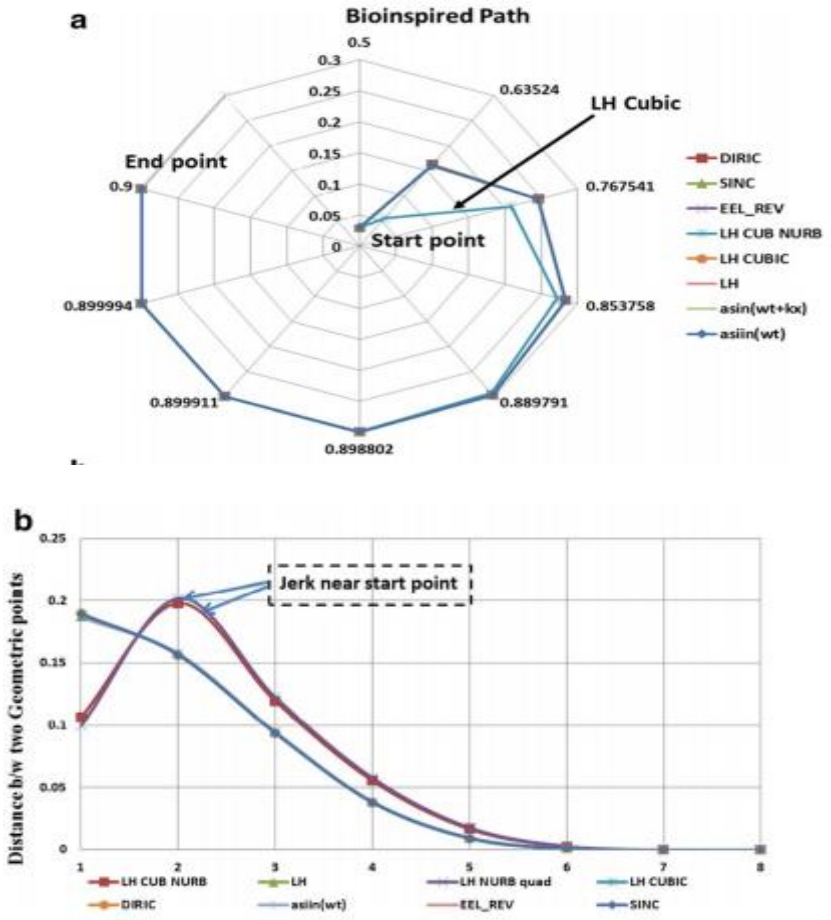

The mathematical equation called Cardinal Sine or Sinc oscillates with equal periodical frequency between positive and negative values describes a sinus wave that reduces by 1/x. Such oscillation reflects an elevated frequency reduction in amplitude. It also indicates that the mean value of one point xim x-0 would be greater than om omi x+, omi omi 0- as well as other osciliating points. This means that the mean value of a point x omi 0 is higher. This function is continuous with a reversible singularity of x=0 at all real values (where 1 is the first derived). Figure 6a revealed two mathematical expressions that were unnormalized (blue) and standardized (red).

The physical meaning can be perceived as a wave signal propagated to a sharp or slow turning motion by a corpse leading to the trailing edge. If one looks at Lighthill's moving wave envelope, sinc fit in to shift the fish body at c speed and with the amplitude c2x + c1x2

that may differ along the fish body with location. The suggested Lighthill Frame undulating motion is presented as

$$y_{body}(x,t) = \left[\left(c_1 x + c_2 x^2\right)\right]\left\{\frac{\sin(kx + 2\pi f \times t)}{2\pi f \times t}\right\}$$

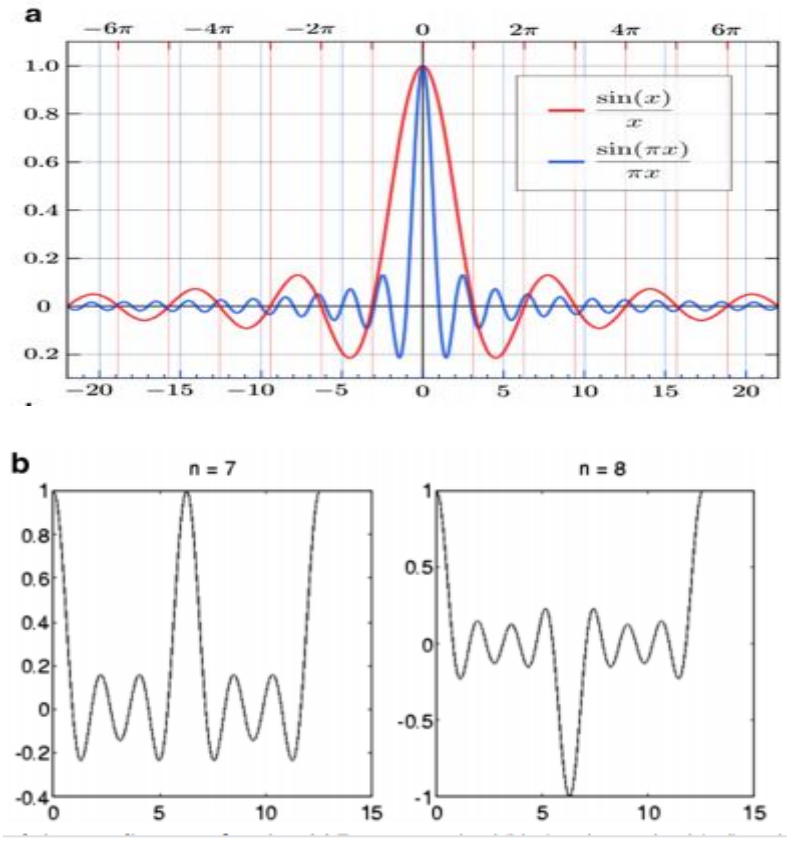

In Table 1, with oscillating waveforms, cubic light hill and cubic NURB (aparticulate to quadratical light hill) the only improvement in the Lighthill wave appears, whereas the two other waves, the oscillating fin and the quadratic NURB wave, are closer but record 1.02 percent and 28.7 percent, respectively more than the quadratic lift distance.

Table 1 Trajectory (geometric) points for mathematical oscillatory/undulatory propulsive waveforms

Node number	Oscillatory sin		LH quad		LH cubic		NURB quad	
	x pos	*y* pos	*x* pos	*y* pos	*x* pos	*y* pos	*x* pos	*y* pos
1 (start point)	0.500000	0.029700	0.500000	0.029700	0.500000	0.029700	0.500000	0.029700
2	0.635240	0.160918	0.634913	0.159944	0.634781	0.159549	0.598402	0.046079
3	0.767541	0.245599	0.767169	0.245283	0.767018	0.245155	0.723631	0.204411
4	0.853758	0.283287	0.853553	0.283192	0.853471	0.283154	0.827144	0.270115
5	0.889791	0.296484	0.889726	0.296460	0.889699	0.296450	0.880214	0.292851
6	0.898802	0.299593	0.898791	0.299589	0.898787	0.299587	0.896969	0.298948
7	0.899911	0.299970	0.899910	0.299969	0.899910	0.299969	0.899745	0.299912
8	0.899994	0.299998	0.899994	0.299998	0.899994	0.299998	0.899982	0.299994
9 (end point)	0.900000	0.300000	0.900000	0.300000	0.900000	0.300000	0.900000	0.300000

4.0 Conclusions

The object of this paper is to translate the BCF mode of biological fish carangi-like swimming behaviour, in order to permit its energy-saving navigation over a certain distance using good balance speed and agility properties. The robotic fish model is combined with the LH statistical model system (kinematics and dynamics). In the LH system, mathematical waveforms are investigated to produce undulatory post-corporal motions. Such functions are paired with the reverse cinematics of the robot, which can create specific bio-inspired pathways for postal robotic fishing movement.

References

1. Triantafyllou MS, Techet AH, Hover FS (2004) Review of experimental work in biomimetic foils. IEEE J Ocean Eng 29:585–594. doi:10.1109/JOE.2004.833216

2. Bullinaria JA (2003) From biological models to the evolution of robot control systems. Phil Trans R Soc A 361:2145–2164. doi:10.1098/rsta.2003.1249

3. Bandyopadhyay PR (2005) Trends in biorobotic autonomous undersea vehicles. IEEE J Ocean Eng 30:109–139. doi:10.1109/JOE.2005.843748

4. Lighthill MJ (1970) Aquatic animal propulsion of high hydro-mechanical efficiency. J Fluid Mech 44:256–301. http://dx.doi.org/10.1017/ S0022112070001830

5. Sfakiotakis M, Lane DM, Davies JBC (1999) Review of fish swimming modes for aquatic locomotion. IEEE J Ocean Eng 24:237–252. doi:10.1109/48.757275

6. Barrett D, Grosenbaugh M, Triantafyllou MS (1996) Optimal control of a flexible hull robotic undersea vehicle propelled by an oscillating foil. IEEE Symposium on Autonomous Underwater Technology, Monterey, CA, pp 1–9, doi:10.1109/AUV.1996.532833

7. VanLehn, K., & van de Sande, B. (2009). Acquiring Conceptual Expertise from Modeling: The Case of Elementary Physics. In K. A. Ericsson (Ed.), The Development of Professional Performance: Toward Measurement of Expert Performance and Design of Optimal Learning Environments (pp. 356–378). Cambridge, UK: Cambridge University Press.

8. Walsh, L. N., Howard, R. G., & Bowe, B. (2007). Phenomenographic Study of Students. Physical Review Special Topics-Physics Education Research, 3(2), 020108.

9. Shin, N., Jonassen, D. H., & McGee, S. (2003). Predictors of well-structured and illstructured problem solving in an astronomy simulation. Journal of research in science teaching, 40(1), 6–33.

10 . Junzhi Y, Min T, Shuo W, Erkui C (2004) Development of a biomimetic robotic fish and its control algorithm. IEEE Trans Syst Man Cybern B Cybern 34:No. 4

11. Motomu N, Norifumi O, Kyosuke O (2003) A study on the propulsive mechanism of a double jointed fish robot utilizing self-excitation control. JSME Int J Series C 46:982–990. doi:10.1299/jsmec.46.982 12. Roy Chowdhury A, Prasad B, Kumar V, Kumar R, Panda SK (2014) Inverse dynamics kinematic control of a bio-inspired robotic-fish underwater vehicle propulsion based on Lighthill's slender body model. IEEE OES MTS OCEANS, Taipei, Taiwan

13. Fossen TI (2011) Handbook of marine craft hydrodynamics and motion control. John Wiley & Sons. doi:10.1002/9781119994138 11. Fu KS, Gonzalez RC, Lee CS (1987) Robotics control, sensing, vision and intelligence. McGraw-Hill New York